*International Research Journal of Environmental Sciences*_____ ISSN 2319–1414
Vol. **10(2),** 1-14, April **(2021)** *Int. Res. J. Environmental Sci.*

Contribution to the study of phosphorus adsorption on the marine sedimentary layer from an artificial marine estuary: Vridi canal (Côte d'Ivoire)

MAHI A. Mahi Arthur, YAO Marcel Konan*, N'DA Samuel and Trokourey Albert
Physical Chemistry Laboratory, UFR SSMT, Félix Houphouët–Boigny University of Cocody Abidjan, B.P. V34 Abidjan, Côte d'Ivoire
yaomarcelkonan@gmail.com

Available online at: www.isca.in, www.isca.me
Received 8th September 2019, revised 21st November 2020, accepted 25th January 2021

Abstract

This work focused on the study of phosphorus adsorption on the marine sedimentary layer from Vridi canal. The first part of this work has lead on the study of phosphorus adsorption kinetics on these sediments and, the second part on the study of phosphorus adsorption isotherms at 25°C on these entities. These studies were carried out under three experimental conditions partially simulating the seasonal physical and chemical characteristics of the waters from this estuary, namely: (E1) pH = 6, Salinity = 5%; (E2): pH = 7; Salinity = 30%; (E3): pH = 8, Salinity = 35%. The experiments were carried out in batch mode. The results have showed that the rate of phosphorus adsorption on these sediments increases from E1 to E3. The kinetics of this reaction are all pseudo-order 2 (Blanchard model). As a result, Blanchard model takes precedence over the diffusion kinetics of this nutrient in these substrates, and those in all the experiments carried out. Langmuir isotherm describes well the experimental isotherms obtained in E2, with favorable adsorption at the different concentrations of the synthetic phosphorus solutions, as illustrated by Hall adimensional number less than 1. The experimental isotherms obtained in E3 are in agreement with Freundlich isotherm, with a favorable adsorption shown by the heterogeneity factor less than 1. A good description of the isotherm obtained in E1 isn't given by these two formalisms, thus reflecting the existence of the different types of sites on these sediments surface, with a considerable difference in adsorption energy depending on their position.

Keywords: Adsorption isotherms; Côte d'Ivoire, eutrophication, phosphorus adsorption, Vridi canal.

Introduction

Because of its properties, phosphorus (P) is one of the essential chemical elements in ecosystems. In addition to its multiple anthropogenic uses, it is fundamental in the physiology of living organisms, where it is involved in DNA, bones and cellular metabolism of plants. Its intensive anthropogenic use has ended up causing severe ecological adverse effects to the entire ecosystem, i.e eutrophication. This ecological phenomenon is responsible of the uncontrolled proliferation of aquatic plants of all kinds in water bodies[1,2]. Nitrogen and P are considered its limiting factors, but P is its controlling factor. This is due to sedimentary biogeochemical cycle of P, which is easily controllable[3,4]. Thus, P study in aquatic ecosystems has always been a major focus, particularly that concerning its adsorption on sediments[5-11].

P adsorption on sediments is linked to very complex processes related to each other. These processes depend both on the waters bodies hydrosystems (topography, hydrology, current, tide, etc.[12,13]) and the biogeochemical reactions (precipitation, ion exchange, adsorption, absorption, assimilation, etc.[14,15]). They are governed by several factors, including temperature, nature and composition of sediments, pH, organic matter and salinity[11,16,17]. According to its concentration and the characteristics of aquatic ecosystems, P can accumulate in high quantity in sediments. As a result, sediments play an important role in the balance, metabolism and dynamic of P[13].

Located in Abidjan district, Vridi canal is the only route between Ébrié system and Atlantic Ocean. This artificial estuary is subject to strong anthropogenic pressures. This fact is translated by its relatively advanced pollution status. For illustration, Yao et al.[18], Yao and Trokourey[19], Yao and Trokourey[20] noted that this estuary has a relatively high level of metallic pollution, with significant ecological risks. Also, the works of N'Da et al.[21] have shown that P level in these superficial sediments are relatively important and likely to show eutrophication. This ecological risk is linked to P presence essentially in particulate bioavailable and authigenic apatite forms. As a prelude to decision-making aimed at protecting this ecosystem for its short or long-term development, it is important to understand some mechanisms of its function mode. It is in this context that this study, dealing with P adsorption on the marine sedimentary layer from this artificial estuary, was carried out. Its main purpose is to determine the P adsorptive capacity of these sediments as a function of salinity, the initial concentration of synthetic P solutions and pH.

Materials and methods

Study area: Vridi Canal is located in Southern Côte d'Ivoire, at exactly 4°0'50" West longitude at the North latitude of 5°15'23". This canal is 2.7km long and 370m wide, with depths ranging from 12 to 15m and pits of 10 to 25m [22]. Due to its position, it has an impressive hydrological network, consists of Ébrié system and Atlantic Ocean on the one hand, and fluvial contributions that the most important of which are Mé coastal river and Comoé river to the East, and Agnéby coastal river to the West on the other hand. Its waters seasons are characterized by five seasons: a hot season (HS) from February to April; a rainy season (RS) from May to July; a great cold season (GCF) from August to September; a flood season (FS) from October to November and a short cold season (SCS) from November to December[20]. The entire area from Ébrié system to Atlantic Ocean has its remarkable biodiversity threatened by the heavy pollution caused by strong anthropic pressures. Indeed, this marine estuary is currently the only real escape route for all kinds of pollutants from the entire Abidjan district to Atlantic Ocean, but also by those drained by fluvial contributions[23]. Also, pollutants of marine origin transit there to reach Ébrié system. So, it is a pollutant hotbed of all kinds. Its hydrological network strongly influences the nature and composition of these superficial sediments. Indeed, Yao et al.[18] noted that its superficial sediments are sandy in general. However, the nature and composition of these sediments differ from its continental entrance to its marine entrance. The superficial sediments from its marine entrance are composed of (2.99±1.51)% of rudites, (92.19±12.50)% of sands and (4.82±0.41)% of clays. Those from its central part are (5.43±2.72)% of rudites, (79.90±8.09%) of sands and (14.6±0.50)% of clays. With regard to the sediments from its continental entrance, they are composed of (0.77±0.39)% of rudites, (52.43±4.38)% of sands and (46.80±1.05)% clay. Thus, there is a decrease in the particle size of these sediments from its marine entrance to its continental entrance[18].

Samples collection and clean-up: In this study, only the superficial sediments from the marine entrance of Vridi Canal were considered, since of marine origin. So, in order to better study P adsorption on the marine sedimentary layer from this estuary as a function of its water seasons, a monthly sample was doing to its marine entrance from April 2014 to March 2015, a collection of 12 samples. The sediment samples were taken 5 cm below the superficial sediments using a Van-Veen grab according to AFNOR X 31-100 standard[24]. After their collection, the sediment samples are immediately stored in polyethylene flasks. In laboratory, they have been previously cleared of coarse elements and then cold-dried by freeze-drying to a constant weight in accordance with AFNOR NF EN ISO 16720 standard[25]. Finally, they are stored in well-dried and tightly closed polyethylene flasks. These flasks are stored in the dark at approximately 20°C.

Synthetic P solutions used in this study: In order to approach the natural conditions of this aquatic ecosystem, three synthetic P solutions have been prepared. Also, they aim to evaluate the influence of pH, the initial concentration of the synthetic P solutions and that of salinity on P adsorption on the marine sedimentary layer from Vridi canal. So, pH and salinity of the synthetic P solutions used in this study are: i. E1: pH = 6 and salinity = 5%, to approach the character of the waters from this estuary in FS where Comoé river settles there; ii. E2: pH = 7 and salinity = 30%, to partially simulate the character of the waters from this estuary in SCS where it is observed the rise of cold marine waters during the small marine upwelling season of Atlantic Ocean in this ecosystem in the presence of Comoé river; iii. E3: pH= 8 and salinity = 35%, to partially characterize the waters from this estuary in the seasons of strong oceanic influences (HS, RS and GCS).

pH of these solutions was adjusted by 0.01M HCl and 0.01M NaOH in presence of the various corresponding salinities. These synthetic P solutions were prepared at various concentrations (0, 0.5, 1, 2, 5, 10, 20 and 50mg/L) from potassium dihydrogen phosphate (K_2HPO_4).

P assay in the tests: Murphy and Riley method[26], standardized by AFNOR NF T90-023[27], was used to assay P concentrations in the various test doing. The spectrophotometer Jenway 7315 UV/Visible was used for this purpose.

Dynamic mode used in this study: The Batch experiment was used to study the kinetics and the determination of P adsorption isotherms on the marine sedimentary layer from Vridi canal. The use of this dynamic mode, common in the realization of such a study, has the following advantages: the repeatability and speed of the implementation of the experiments as well as their large-scale realization; the possibility of studying the mobility of P on highly evolved sediments; the possibility of comparing P adsorption capacities on many sediment or soil samples and; the determination of the different adsorption mechanisms of this nutrient on theses substrates[28].

Experimentations of P adsorption kinetics: The study of P adsorption kinetics was carried out taking into account the seasonal nature of the waters from this canal. So, 4g of the sediment samples were placed in contact with 200 ml of each synthetic P solutions at different concentrations (0.5, 1, 2, 5, 10, 20 and 50mg/L) in 250ml Erlenmeyer flasks. These flasks were stirred at 300 rpm to simulate the strong hydrodynamism of this estuary. At regular time intervals (0, 15, 30, 60, 90, 120, 150, 180, 210, 240, 300, 360, 420, 480, 540, 600, 660, 720min), 10 ml of the test were collected and filtered on Whatman filter paper. The instantaneous P amount adsorbed on the sediments at time t (q (t)) is given by:

$$q(t) = (C_i - C_t)\frac{V}{m} \quad (1)$$

with C_i and C_t, P initial concentration and P concentration at time t in the solution test respectively; V, volume of the synthetic P solutions; m, mass of sediment samples.

Determination of the pseudo-order of P adsorption kinetics: For the determination of the pseudo-order of P adsorption kinetics on the marine sedimentary layer from Vridi canal, the characteristics of the plot of log (qe-q (t)) as a function of t (2) were used for Lagergren model[29] (pseudo-order 1) and the plot of $\frac{t}{q(t)}$ as a function of t (3) for Blanchard model[30] (pseudo-order 2).

$$\mathrm{Log}\big(q_e - q(t)\big) = \log(q_e) - \frac{k_1}{2{,}303}t \quad (2)$$

$$\frac{t}{q(t)} = \frac{1}{k_2 q_e^2} + \frac{1}{q_e}t \quad (3)$$

With q(t) and q_e (mg/g), P amount adsorbed by the sediment samples layer at the time t and at equilibrium respectively; k_1, the kinetic rate constant of pseudo-order 1(t^{-1}); k_2, the kinetic rate constant of pseudo-order 2 ($mg^{-1}t^{-1}$).

Of these two models, the best is that simultaneously presenting the high correlation coefficients (R) and the low differences between theoretical q_e values and the experimental q_e values.

Diffusion kinetics models used for the characterization of P adsorption kinetics: Two kinetic diffusion models were used in this study: the external diffusion model and the intraparticular diffusion model. For the external diffusion model, the plot of ln (1-F) as a function of t (4)[31,32] was used to characterized this diffusion. Concerning the intraparticular diffusion model, it was used Weber and Morris model[33], namely the plot of q(t) as a function of $t^{\frac{1}{2}}$ (5).

$$\ln(1 - F) = -k_{fd}\,t \quad (4)$$

$$q(t) = k_d t^{\frac{1}{2}} + c \quad (5)$$

with $F = \frac{q(t)}{q_e}$; k_{fd} (t^{-1}), the external diffusion constant; k_d, ($mg/g.h^{1/2}$) the intraparticular diffusion constant.

If the diffusion kinetics is intraparticular then the plot of q (t) as a function of $t^{1/2}$ is a straight line with a high correlation coefficient (R> 0.900), while if it's external the plot of -ln (1-F) as a function of t is a straight line, and that also with a high correlation coefficient (R> 0.900).

Determination of the experimental adsorption isotherms: The studies leads on P retention on sediments with batch mode show that the equilibrium is usually reach between 4 and 48 h[4;11]. Thus, the experimental adsorption isotherms were carried out for 48 h, at the room temperature (25±1°C), because the water temperatures changes very slightly in Vridi canal and is very close to that of air ambient temperatures. The tests were carried out under the same conditions as that of the study of P adsorption kinetics, with the difference that P concentrations at the equilibrium is evaluated after 48 h. P amount at the equilibrium (qe) (mg/g) is obtained as follows:

$$q_e = (C_i - C_e)\frac{V}{m} \quad (6)$$

with C_i and C_e, P initial concentration and P concentration at the equilibrium in the solution tests respectively; V, volume of the synthetic P solutions; m, mass of the sediment samples.

Characterization of the experimental adsorption isotherms: The experimental adsorption isotherms obtained were characterized using the classification of Giles et al.[34] and that of Brunauer[35].

Experimental adsorption isotherms modeling by Langmuir and Freundlich isotherms: The modeling of experimental adsorption isotherms was doing first by Langmuir isotherm[36] using its five linear forms (from 7 to 11)

(L1) $$\frac{1}{q_e} = \frac{1}{q_m} + \frac{1}{q_m K_L} \times \frac{1}{C_e} \quad (7)$$

(L2) $$\frac{C_e}{q_e} = -\frac{1}{K_L q_m} + \frac{1}{q_m} \times C_e \quad (8)$$

(L3) $$q_e = -\frac{1}{K_L}\frac{q_e}{C_e} + q_m \quad (9)$$

(L4) $$\frac{q_e}{C_e} = -K_L q_e + K_L q_m \quad (10)$$

(L5) $$\frac{1}{C_e} = K_L q_m \frac{1}{q_e} - K_L \quad (11)$$

With: q_e, P amount taken by the sediment samples at the equilibrium (q_e) (mg/g); q_m, P maximum amount taken by sediment (q_m) (mg/g); C_e, P concentration at the equilibrium in the solution tests; K_L (L/g) the Langmuir constant.

The best of these linear forms leading to a better approach of the experimental adsorption isotherms was chosen taking into account the following conditions: i. this model must have a strong correlation R ($R \geq 0.900$) with the experimental data; ii. the Root Mean Square Error must be inferior at 10% and be the lowest.

The assessment of the adsorption capacity of Langmuir isotherm[36] corresponding at best to the experimental adsorption isotherms has been doing by the adimensional number of Hall (R_L)[37]:

$$R_L = \frac{1}{1 + K_L C_i} \quad (12)$$

with: K_L, (L/g) the Langmuir constant; C_i, P initial concentration in the solution tests.

Thus, the adsorption is: irreversible for $R_L = 0$; favorable for $0 < R_L < 1$; linear for $R_L = 1$; unfavorable for $R_L > 1$.

The experimental adsorption isotherms were then modeling by Freundlich isotherm[38]. As for this isotherm model, its linear form (13) was used.

$$\ln q_e = \ln K_F + \frac{1}{n_f} \ln C_e \quad (13)$$

With: q_e, P amount taken by the sediment samples at the equilibrium (q_e) (mg/g); C_e, P concentration at the equilibrium in the solution test; K_F (L/g) the Freundlich constant; $\frac{1}{n_f}$, the heterogeneity factor.

If $\frac{1}{n_f}$ is unity, the adsorption is linear.

This means that the adsorption sites are homogeneous (as in the Langmuir isotherm[37]) from the energy point of view and no interaction takes place between the adsorbate and the adsorbent. If the value of $\frac{1}{n_f}$ is smaller than 1, the adsorption is favorable; and the sorption capacity increases in this case with the production of new adsorption sites. When the value of $\frac{1}{n_f}$ is greater than 1, the adsorption link becomes weak. The adsorption is unfavorable due to decreases in adsorption capacity[39].

The choice conditions for this formalism to describe the experimental isotherms obtained were the same as those used in the case of Langmuir isotherm[36].

Results and discussion

Study of the simultaneous effect of pH, salinity and P initial concentration on P adsorption kinetics: All plots of q = f (t) generally have the same profile. Two distinct characteristics were noted in P adsorption kinetics on the marine sedimentary layer from Vridi Canal. The first was characterized by two phases and, the second by three phases. Concerning P adsorption kinetics characterized by two phases, it was observed in E1 and E2 for C_i = 0.5; 2; 20 and 50mg/L, E2 and E3 for C_i = 5mg/L, and simultaneously in the three experiments (E1, E2 and E3) for C_i = 10mg/L. In these cases, the equilibrium time is reached after 0.25h. Thus, it was observed a fast kinetics between 0 and 0.25h, followed by the pseudo equilibrium phase beyond 0.25h. For P adsorption kinetics characterized by three phases, it was observed in E1 for C_i = 5mg/L, E3 for C_i = 0.5; 2; 20 and 50mg/L, and simultaneously in the three experiments (E1, E2 and E3) for C_i = 1mg/L. Except in E3 for C_i = 0.5mg/L where the equilibrium time was obtained after 2h, all other cases have the equilibrium time after 0.5h. As a result, there was observed almost negligible P adsorption between 0 and 0.25 h (between 0 and 2h in E3 for C_i = 0.5mg/L). This fact was followed by its rapid adsorption between 0.25 and 0.5h for C_i = 0.5 and 5mg/L in E1, for C_i = 20 and 50mg/L in E3, and in all experiments for C_i = 1mg/L and between 2 and 2.5h for C_i = 0.5 mg/L in E3. It follows a pseudo equilibrium phase after this step (Figure-1). qe increases with C_i in all the experiments carried out. It is the same case from E1 to E3, except for $C_i \leq$ 1mg/L (Table-1).

The profiles of P adsorption kinetics on the marine sedimentary layer from Vridi canal are generally similar to those obtained by Hei et al.[6], Huang et al.[7], Huang et al.[8], Li et al.[9] and Bai et al.[11] in similar studies.

The different equilibrium times, mostly less than 1 h, illustrate a rapid reactivity of P with respect to these sediments. This fact has been noted by Chmielewka et al.[40], concerning the kinetics of P retention on materials of natural origin (the equilibrium time less than 60min) such as montmorillonite, zeolite, alginate. qe values observed in this study are higher than those obtained by Cao et al.[5] from the study of P adsorption on the marine sedimentary layer from Sanggou Bay and, to those of Meng et al.[10] on the marine sedimentary layer from Changjiang Estuary. On the other hand, they are very low compared to those obtained by Bai et al.[11] in such a study with the marine sedimentary layer from Yellow River Delta (China). An increase in P concentrations in solution would favor a collision between phosphate ions and the active sites of these sediments[39].

This process would explain the increase of q_e with C_i in all different experiments carried out. This observation confirms the influence of qe on P retention by substrates as a function of the concentration gradient[41-43]. Thus, this process would show the existence of external resistance to mass transfer due to the external film (access to Gouy-Chapman diffusion limit layer[44]). This resistance decreases with the increase of the concentration gradient and with that of the agitation time[39]. This phenomenon, coupled with some physical and chemical process, explains some particularities observed in this study. Indeed, its coupling with P remobilization from its apatite forms[20;39] could explain the low adsorption of this nutrient for values for $C_i \leq$ 1mg/L in E1 with respect to E2 and E3. Also, they would cause the very low P adsorption (almost zero) in E1 for C_i = 0.5; 1 and 5mg/L between 0 and 0.5h. This mass transfer resistance with the high salinity would also impact P adsorption in E2, almost zero for C_i = 1mg/L between 0 and 0.25 h. Also, its simultaneous coupling to the high salinity[11;45] and the basicity of the synthetic P solutions (initial competition between the hydroxide ions (OH-) and phosphate ions on the various adsorption sites[39]) in E3 would inhibit P adsorption for C_i = 0.5 between 0 and 1.5 h, and C_i = 1; 2; 20 and 50mg/L between 0 and 0.5h. In general, it was noted a rapid adsorption of phosphate ions in solution on these sediments surface (the first stage of the two-phase kinetics and the second stage of the three-phase kinetics), followed by their gradual adsorption. This adsorption is similar to the retention in the channels or pores of materials (diffusion phenomenon) (the second stage of the two-phase kinetics and the third stage of the three-phase kinetics). The observations noted by Liu et al.[45] on the decay of P adsorption on sediments for pH between 6 and 8 were confirmed in this study, and this by the decay of qe from E1 to E3.

Table-1: Evolution of P concentration at equilibrium (qe) as function of P initial concentrations (C_i).

Parameters			P initial concentration (C_i (mg/L))						
			0.5	1	2	5	10	20	50
E1	pH = 6 salinity = 5%	qe (mg/g)	0.100	2.720	15.228	24.410	36.172	103.261	113.34
E2	pH = 7 salinity = 30%		0.679	4.742	5.766	25.1	33.553	44.118	51.627
E3	pH = 8 salinity = 35%		0.650	3.633	6.001	28.34	34.42	45.360	56.253

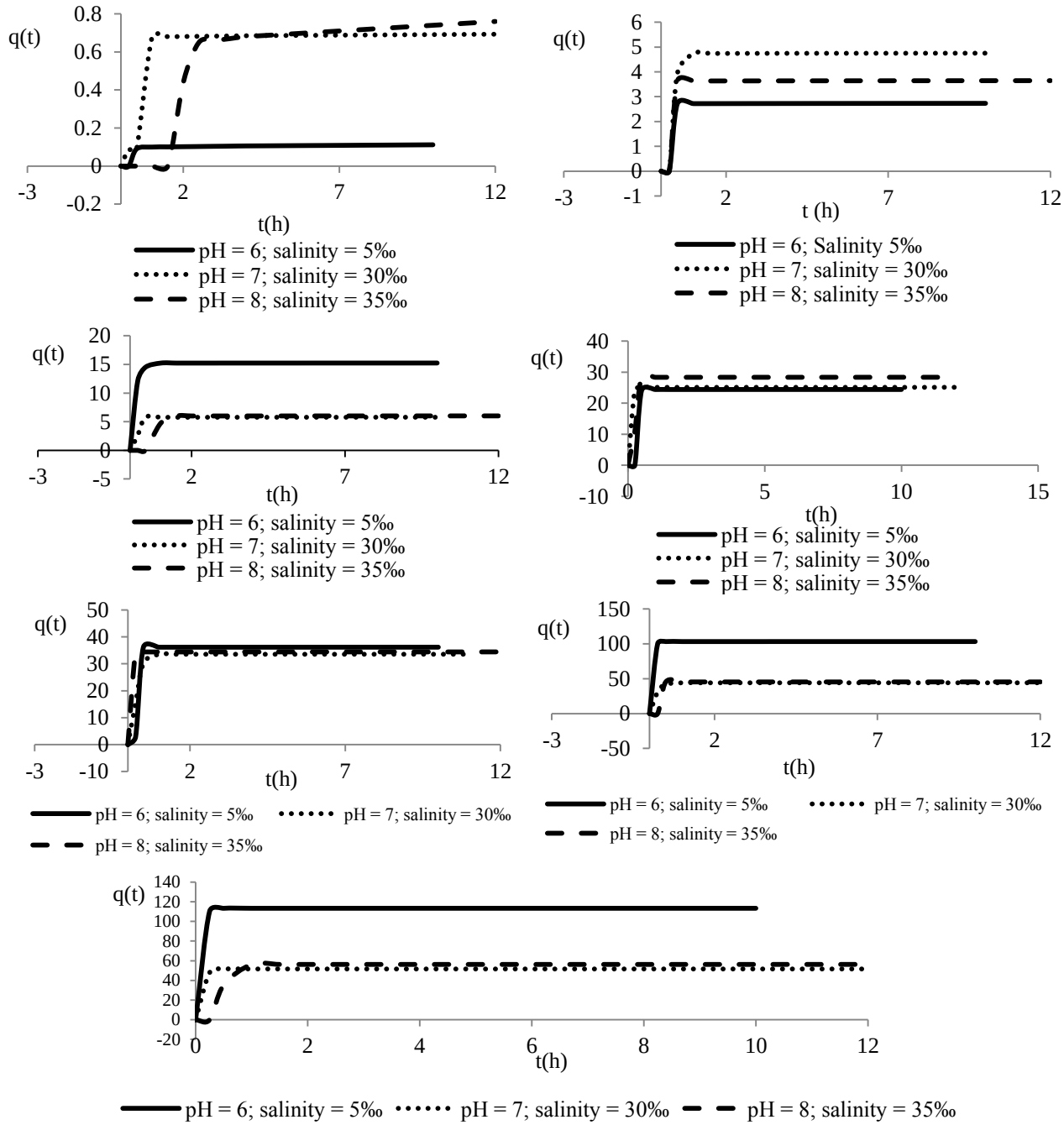

Figure-1: P amount adsorbed by the sediment samples from Vridi canal at the time t (q(t)) as a function of t for the different P initial concentrations.

In the end, it appears from the results obtained that P retention depends on pH, concentration and salinity of the initial synthetic P solutions. Thus, these parameters would influence not only phosphate ions speciation in solution, but also the nature of minerals surface charges constituting these sediments. This strong influence of these parameters on this phenomenon shows that it is due to electrostatic interactions (attraction/repulsion), chemical and/or ligand exchange. These types of reactions were mentioned by Coulibaly[39]. In addition, these results obtained are in according with those of N'Da et al.[21]; which noted a relatively high presence of P in the superficial sediments from Vridi Canal in the presence of Comoé River (natural conditions partially simulated by E1) compared to the seasons when the influence of Atlantic Ocean is very important (partially simulated natural conditions by E2 and E3). Therefore, it is concluded the fundamental importance of pH, salinity and P flux contributions in the dynamics of this nutrient in the marine sedimentary layer from this artificial estuary.

Kinetics adsorption modeling by Largergren and Blanchard models: The characteristics of Lagergren model (pseudo order 1)[29] and Blanchard model (pseudo order 2)[30] obtained from the experimental data are given in Table 2. R values obtained with Lagergren model[28], between 0.308 and 0.946, are relatively low in most cases. It is the same for its theoretical qe compared to the experimental qe. Regarding R values for the Blanchard model[30], they are all important (between 0.946 and 1). Also, the theoretical qe obtained with this model have a low difference with the experimental q_e. The initial rates of P adsorption on these sediments are very important in Blanchard model[30] compared to those obtained by Lagergren model[29]. From these results, it appears that P adsorption on the marine sedimentary layer from Vridi canal can't be translated by Lagergren model[29]. Thus, the rate of this reaction doesn't depend only on P concentration in the synthetic solutions. It would involve other parameters as suggested by its relevance to Blanchard model[30]. The similar results have been obtained by Coulibaly[39] in the case of the study of P adsorption on geomaterials and, by Bai et al.[11] in a similar study with soils originating from "Yellow River Delta" (China). The acuteness of Blanchard model[30] to describe such processes would be based on taking into account the real heterogeneity of complexation sites[39].

Table-2: Characteristics of Largergren and Blanchard models applied to the experimental data in this study.

Parameters	Model	Rate	P initial concentration (C_i)						
			0.5	1	2	5	10	20	50
pH = 6; Salinity = 5‰	Largergren model	k_1	0.368	0.530	0.677	0.719	0.666	0.633	0.603
		$q_{e,cal}$	0.031	0.095	0.246	0.314	0.223	0.180	0.244
		R^2	0.756	0.516	0.564	0.516	0.431	0.431	0.429
		R	0.892	0.718	0.751	0.718	0.657	0.657	0.655
	Blanchard model	k_2	9.490	66.613	4.225	20	0.052	8.100	6.40
		$q_{e,cal}$	0.113	2.740	15.385	25	40	111.111	125
		R^2	0.999	1	1	1	0.956	1	1
		R	0.999	1	1	1	0.978	1	1
pH = 7; Salinity = 30‰	Largergren model	k_1	0.442	0.712	0.599	0.274	0.723	0.113	0.541
		$q_{e,cal}$	0.095	0.231	0.115	0.104	0.424	4.199	9.423
		R^2	0.648	0.588	0.504	0.465	0.526	0.514	0.496
		R	0.308	0.767	0.710	0.465	0.725	0.489	0.704
	Blanchard model	k_2	1.331	8.740	2.924	15.21	0.841	4.840	5.157
		$q_{e,cal}$	0.774	4.785	5.848	26.641	34.483	45.455	52.632
		R^2	0.946	0.999	0.999	1	0.999	1	1
		R	0.946	0.999	0.999	1	0.999	1	1
pH = 8; Salinity = 35‰	Largergren model	k_1	0.378	0.442	0.654	0.518	0.382	0.548	0.696
		$q_{e,cal}$	0.640	0.094	0.469	0.163	0.060	0.201	0.601
		R^2	0.894	0.503	0.616	0.435	0.380	0.416	0.491
		R	0.946	0.709	0.785	0.435	0,616	0.645	0.701
	Blanchard model	k_2	1.278	3.754	2.723	0.673	7.84	4.84	2.890
		$q_{e,cal}$	0.816	3.650	6.061	28.571	35.714	45.455	58.824
		R^2	0.994	1	0.999	0.999	1	1	0.999
		R	0.997	1	0.999	0.999	1	1	0.999

With: $q_{e,cal}$, theoretical qe ($mg.g^{-1}$); k_1, the kinetic rate constant of pseudo-order 1(t^{-1}); k_2, the kinetic rate constant of pseudo-order 2 ($mg^{-1}t^{-1}$).

P kinetics adsorption modeling by intraparticular and external diffusion models in this study: The characteristics of the external diffusion model and the intraparticular diffusion model obtained from the experimental data are given in Table 3. The plots of the experimental data according to the equations of these diffusion models are not straight lines (Figures 2 and 3). The different linear correlation coefficients R (between 0.329 and 0.868 for the intraparticular diffusion model, and between 0.311 and 0.894 for the external diffusion) are relatively low. Thus, the diffusion isn't the only mechanism limiting P adsorption on the marine sedimentary layer from this artificial estuary. There are two linearities in the diffuse modeling of this kinetics: one before the equilibrium (first step) and the other after the equilibrium (second step). This fact suggests two steps in the diffusion of this adsorption process. The diffusion phenomena have a particular importance with the increase of C_i.

In the case of external diffusion, the results obtained show that P external diffusion in the film around the adsorbent particles (boundary layer) wouldn't limit the adsorption process. So, the agitation rate applied during the batch mode tests isn't sufficient to break the resistance exerted by the boundary layer to the transfer of phosphate ions to the sediments surface. Thus, is it to confirm the existence of an external resistance to mass transfer due to the external film (access to Gouy-Chapman diffusion limit layer[44]). This external resistance decreases with increasing concentration gradient and stirring time, as already be noted during the study of the simultaneous influence of pH, salinity and initial concentration on the kinetics of P adsorption on these marine sedimentary layer. As noted by Djelloul[46], the first step of the external diffusion is related to the rapid migration of phosphate ions in the different interparticle spaces, followed by the second step which concerns a slow migration in these spaces. This external diffusion is influenced by intraparticular diffusion, which doesn't also limit P adsorption kinetics on these sediments. This distribution is also done in two stages. According to Coulibaly[39] and Chmielewska[40], the first step of the intraparticle diffusion corresponds to an instantaneous fixation of phosphate ions on the reactive sites (instant adsorption), and the second step relates to the slow diffusion of these ions to the inside pores (gradual adsorption). The increasing of k_d (the intraparticular diffusion coefficient) with C_i shows that P transfer to the active sites inside the pores by diffusion accelerates this process. This process is therefore instantaneous for the high initial concentrations of P[39]. Karaca et al.[47] explain the increase of k_d with that of C_i is due to the intensification of the driving forces created by the interactions between phosphate ions. These forces would reduce external diffusion and promote intraparticular diffusion. This fact could explain the simultaneous observation of the two stages in these diffusions. It may therefore be suggested that rapid external diffusion is followed by the rapidity of intraparticular diffusion before the equilibrium time. The progressive saturation of the pores by P retention would affect the intraparticular diffusion, which becomes slow. This fact would have repercussions on the external diffusion, which itself becomes slow also: it would be reached the equilibrium. These observations in this study on the intraparticular diffusion have also been doing in several studies, including that by Masmoudi et al.[48] concerning the use of activated carbons for the mercury removal of in aqueous solution, and those of Ouakouak and Youcef[49] in the study of Cu^{2+} adsorption on activated carbon and bentonite.

In the end, it appears from these results that Blanchard model[30] take precedence over that of diffusion in this study.

Table-3: Characteristics of external and intraparticular diffusion models obtained from the experimental data in this study.

Parameters	Model	Rate	P initial concentration (C_i)						
			0.5	1	2	5	10	20	50
pH = 6; Salinity = 5‰	Intraparticular diffusion model	k_d	0.027	0.615	2.334	5.501	7.852	13.72	15.04
		C	0.041	1.267	9.795	11.34	17.55	71.66	78.71
		R^2	0.537	0.406	0.347	0.406	0.407	0.264	0.263
		R	0.733	0.637	0.589	0.637	0.638	0.514	0.513
	External diffusion model	k_{fd}	0.325	0.325	0.219	0.18	0.106	0.069	0.061
		R^2	0.799	0.361	0.300	0.235	0.213	0.131	0.126
		R	0.894	0.601	0.548	0.485	0.462	0.362	0.355
pH = 7; Salinity = 30‰	Intraparticular diffusion model	k_d	0.169	1.18	1.094	2.845	5.99	6.127	1.028
		C	0.249	2.011	3.726	18.08	19.15	28.84	43.62
		R^2	0.514	0.463	0.408	0.242	0.424	0.343	0.108
		R	0.717	0.680	0.639	0.492	0,651	0.586	0.329
	External diffusion model	k_{fd}	0.12	0.332	0.213	0.092	0.17	0.125	0.103
		R^2	0.341	0.366	0.245	0.148	0.283	0.244	0.169
		R	0.584	0.605	0.495	0.385	0.532	0.494	0.411
pH = 8; Salinity = 35‰	Intraparticular diffusion model	k_d	0.274	0.704	1.649	4.567	3.805	8.738	12.31
		C	0.042	1.861	1.716	16.88	25.08	23.27	24.80
		R^2	0.753	0.372	0.539	0.371	0.228	0.368	0.463
		R	0.868	0.610	0.734	0.609	0.477	0.607	0.680
	External diffusion model	k_{fd}	0.099	0.356	0.311	0.171	0.062	0.238	0.15
		R^2	0.330	0.453	0.411	0.200	0.097	0.210	0.284
		R	0.574	0.673	0.641	0.447	0.311	0.458	0.533

With: k_d (the intraparticular diffusion coefficient) ($mg.g^{-1}.h^{-1/2}$); k_{fd} (the external diffusion coefficient) (t^{-1}); C (mg/g).

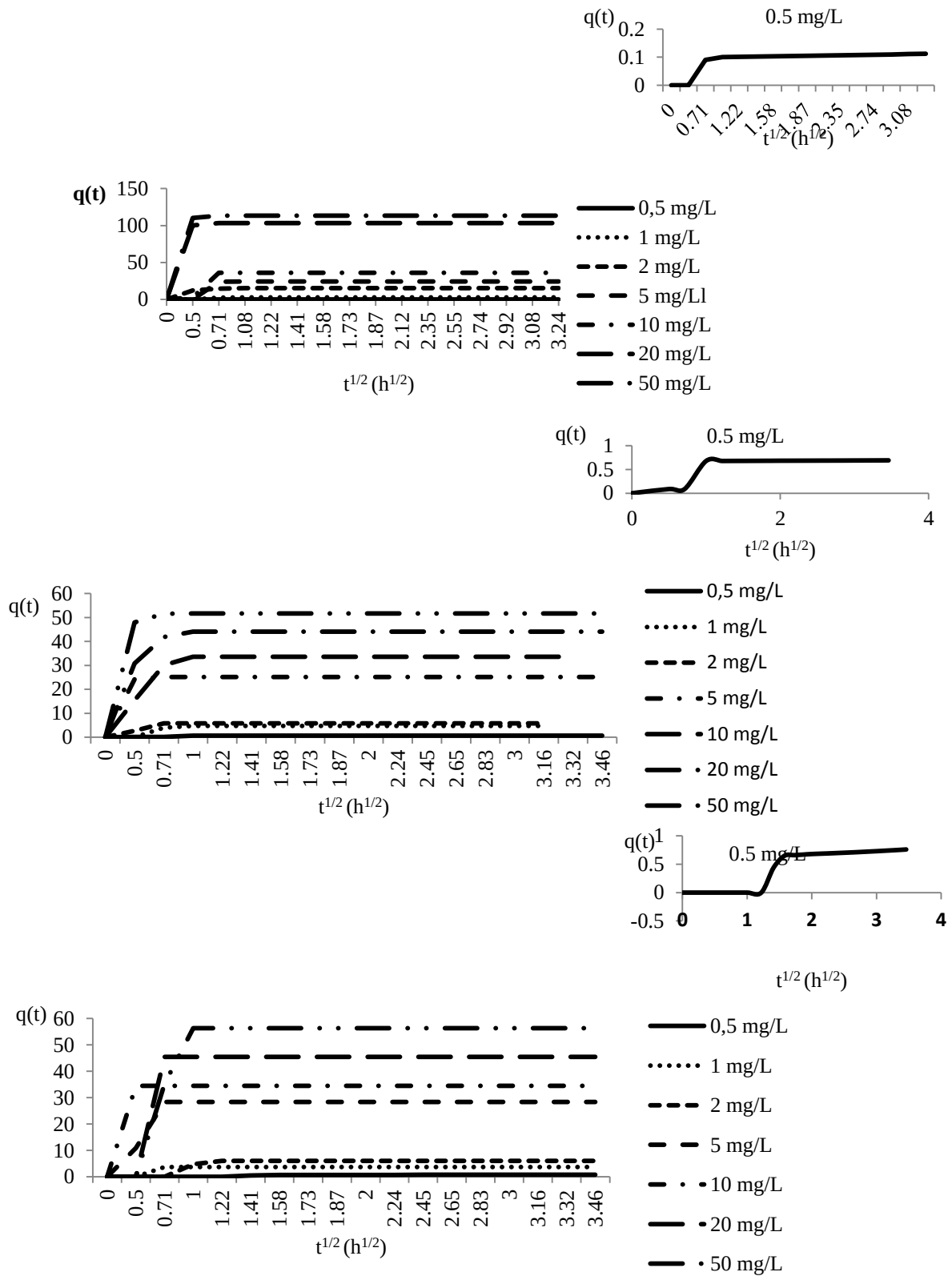

E3 (pH = 8; Salinité = 35‰)

Figure-2: Plot of the experimental data for the intraparticular diffusion model from the experimental data in this study.

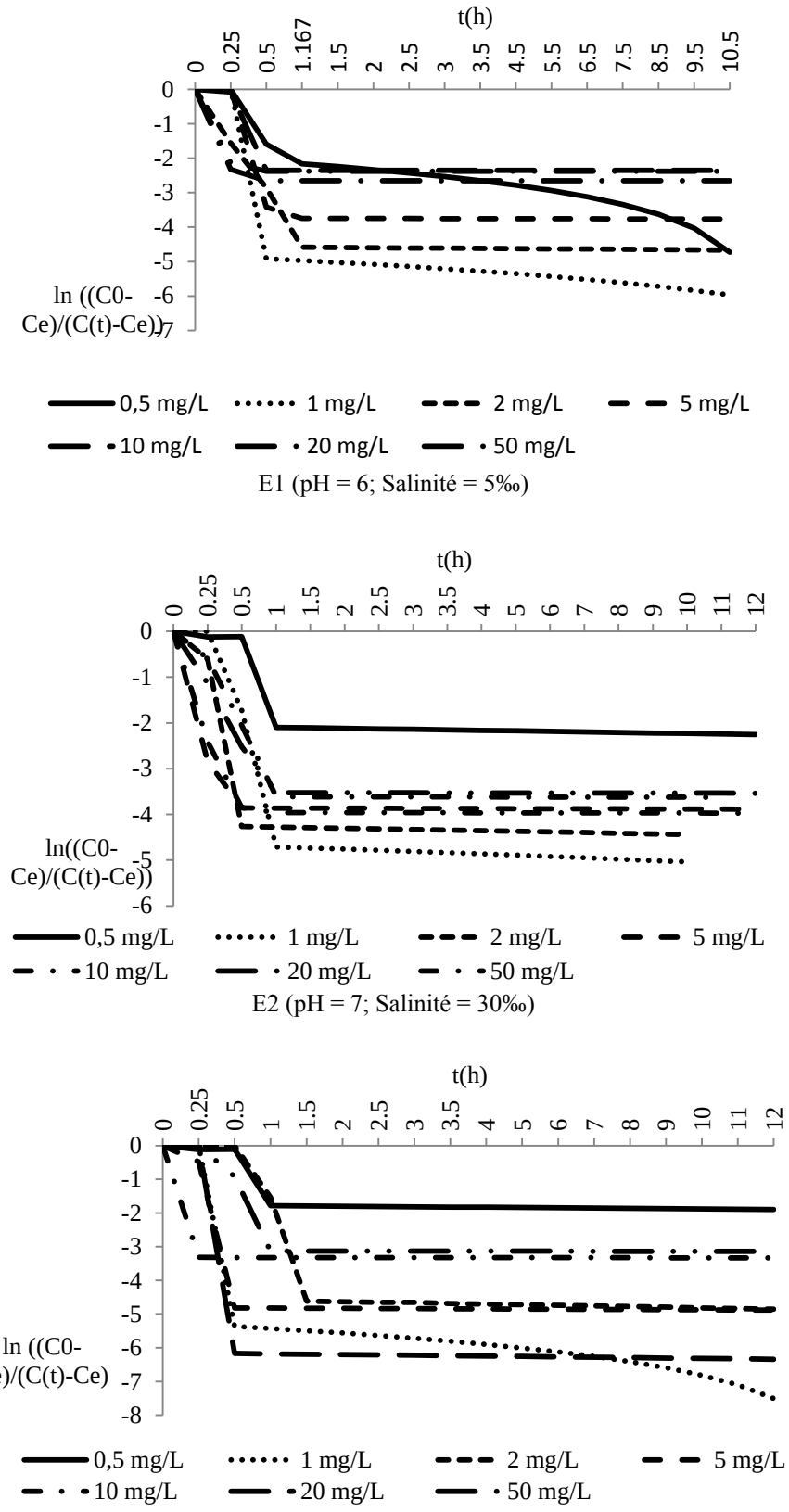

Figure-3: Plot of the experimental data for the external diffusion model from the experimental data in this study.

Classification of the experimental adsorption isotherms: The experimental adsorption isotherms obtained in this study are all of type L2 in the classification of Giles et al.[34] and type I according that of Brunauer[35] (Figure-4). This type of isotherm is characterized by a rapid increase in the adsorbed amount in the range of low equilibrium concentrations followed by an approximately horizontal plateau to the saturation vapor pressure obtained at high concentrations. This isotherm is generally attributed to adsorption on a surface with micropores[35]. According to Giles et al.[34], this type of isotherm is the most common for such studies. It is characterized by slow adsorption as the degree of recovery increases. The adsorption in this type of isotherm is done by progressive occupation of the available sites until saturation[39]. Therefore, no more retention occurs once these sites are occupied (establishment of the monolayer). In the case of P adsorption by this isotherm, more explications are given by Barrow[50]. According to this author, when an orthophosphate anion adsorbs specifically on a surface, the surface electric charge increases and the reaction with an additional orthophosphate anion molecule becomes less easy. There is therefore a decrease in the affinity of a surface for orthophosphate anion with its adsorption.

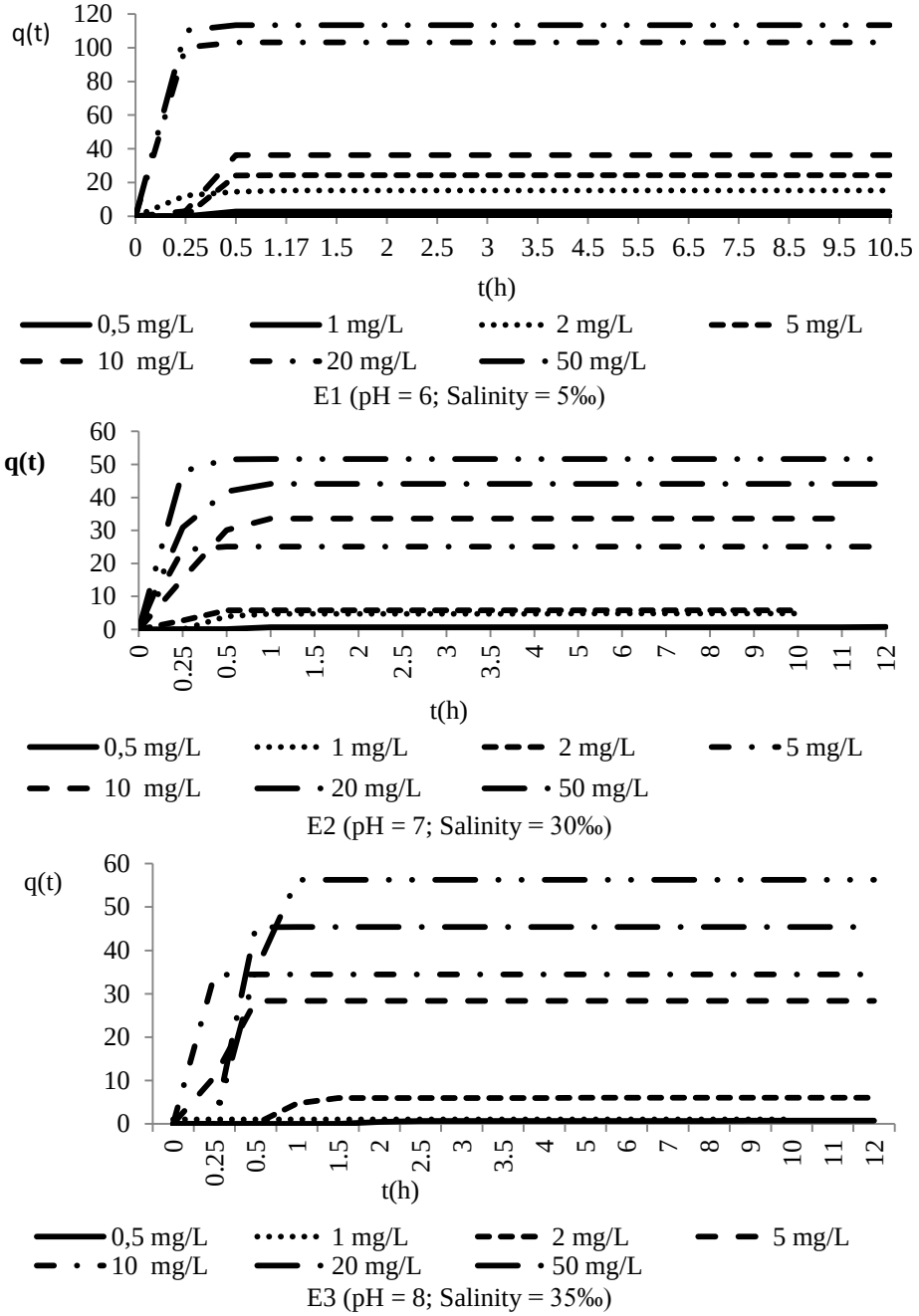

Figure-4: Experimental isotherm obtained in this study at 25°C.

Experimental adsorption isotherms modeling by Langmuir and Freundlich isotherms: The application of the five linear forms of Langmuir isotherm[36] to the experimental data shows that L1 leads to a better approach of the experimental adsorption isotherms. This fact is reflected by the strong correlations observed between L1 and the experimental data, unlike the other four linear forms of this model (Table-4). Comparing these results with those obtained with Freundlich isotherm[38] (Table-5), the following remarks are doing: i. these two models of isotherm, although having a relatively good correlation with the experimental data, don't give a good description of the experimental adsorption isotherms obtained in E1, because of their too high RMSE; ii. Langmuir isotherm (L1), with a correlation close to 1 and a very low RMSE (<10%) is more suitable than Freundlich isotherm for the experimental adsorption isotherm modeling obtained in E2; iii. Freundlich isotherm has good sharpness compared to that of Langmuir (L1) for the description of the experimental adsorption isotherms obtained in E3, because it has the lowest RMSE despite its R value lower than that obtained from Langmuir model (L1).

On the other hand, the adimensional number of Hall (R_L)[37] decreases with C_i in E2 and is less than 1 for all these concentrations (Table-6).

The capacity of L1 to approach the experimental results compared to the four other linear forms of Langmuir isotherm in this study are in agreement with the results obtained by Djelloul[46] in the framework of textile effluents elimination by milk thistle seeds. This fact would justify the great frequency of the application of this linear form of Langmuir isotherm for experimental adsorption isotherms modeling in solid-liquid adsorption phenomena, particularly that of P adsorption on substrates[6-8;39;41;43]. The good modeling of the isotherm obtained in E2 by the Langmuir model would indicate that the experimental conditions used favor the majority development of homogeneous adsorption sites on these sediments surface[49]. Thus, it would have a direct contact of phosphate ions with these sediments surface up to the monolayer cover[49;51]. R_L values show that this adsorption is favorable[37]. Regarding E3, the good modeling of its experimental adsorption isotherms by Freundlich isotherm would illustrate the majority development of heterogeneous adsorption sites[49] on these sediments surface, favored by the experimental conditions. n_f value greater than 1 in this experiment indicates that P adsorption is favorable on these sediments surface under the experimental conditions implemented in E3[46]. The non-adequacy of Freundlich and Langmuir isotherms to model the experimental adsorption isotherms obtained in E1 is explained by the biogeochemical reactions complexity (such as the release of P from its apatite forms[8], exchangeable acidity[11], etc.) that take place under the established experimental conditions. In addition, the high values of R obtained for these two isotherm models in this experiment, would indicate a relatively important and simultaneous development of homogeneous and heterogeneous adsorption sites. As a result, the experimental conditions used in E1 would lead to the existence of different types of sites on these sediments surface, with a considerable difference in adsorption energy depending on the site position. This observation was underlined by Jiang et al.[52] in the case of clay.

Table-4: The characteristics of the five linear forms of Langmuir isotherm obtained from experimental data in this study.

Parameters	Rate	Linear forms of Langmuir model				
		L1	L2	L3	L4	L5
E1 pH=6; Salinity = 5%	K_L	-0.627	-0.01	-0.338	-0.078	-0.675
	q_m	-1.170	-27.027	5.107	118.128	-1.037
	R^2	0.978	0.104	0.233	0.233	0.956
	R	0.956	0.322	0.483	0.483	0.978
	RMSE	61.411	56.696	38.032	56.423	60.058
E2 pH=7; Salinity = 30%	K_L	0.85	1.133	2.053	0.369	-3.128
	q_m	58824	58.824	34.91	86.260	0.388
	R^2	0.998	0.981	0.180	0.180	0.025
	R	0.996	0.990	0.424	0.424	0.158
	RMSE	0.582	32.379	29.839	19.981	27.932
E3 pH=7; Salinity = 30%	K_L	5.25	3.4	12.346	0.951	-6.457
	q_m	47.619	58.824	28.960	76.688	0.474
	R^2	0.998	0.984	0.077	0.077	0.017
	R	0.997	0.992	0.277	0.277	0.130
	RMSE	9.449	37.809	19.180	32.145	27.460

Table-5: the characteristics of the Freundlich isotherms obtained from the experimental data.

Model	Rate	E1 pH = 6; Salinity = 5%	E2 pH = 7; Salinity = 30%	E3 pH = 8; Salinity = 35%
Modèle de Freundlich	$1/n_F$	1.612	0.584	0.405
	n_F	0.620	1.172	2.469
	K_F	7.135	20.843	30.938
	R	0.951	0.973	0.969
	R^2	0.905	0.947	0.938
	RMSE	95.896	8.091	9.276

Table-6: Evolution of the adimensional number of Hall (R_L) according to C_i of synthetic P solutions.

Ci (mg/L)	0.5	1	2	5	10	20	50
R_L	0.702	0.541	0.370	0.190	0.105	0.056	0.023

Conclusion

This study has once again illustrated the individual and simultaneous influence of salinity, pH and phosphorus flux in P adsorption on sediments. It also shows in a general way that the development and the nature of the adsorption sites is a function of the physical and chemical characteristics of aquatic ecosystems, which condition the various complex processes of adsorption. This is the case of Vridi canal.

References

1. Dai, W., Zhang, J., Tu, Q., Deng, Y. and Xiong, J. (2017). Bacterioplankton assembly and interspecies interaction indicating increasing coastal eutrophication. *Chemosphere*, 177, 317-325.

2. Gieswein, A., Hering, D. and Feld, C.K. (2017). Additive effects prevail: The response of biota to multiple stressors in an intensively monitored watershed. *Sci. Tot. Environ*., 593–594, 27-35.

3. Trannum, H.C., Gundersen, H., Oug, E., Rygg, B. and Norderhaug, K.M. (2018). Soft bottom benthos and responses to climate variation and eutrophication in Skagerrak. *J. Sea Res*., 141, 83-98.

4. Wang, Y., Li, Y., Luo, X., Ren, Y., Gao, E. and Gao, H. (2018). Effects of yttrium and phosphorus on growth and physiological characteristics of Microcystis aeruginosa. *J. Rare Earths*, 36(7), 781-788.

5. Cao, X., Zhu, J., Lu, M., Ge, C., Zhou, L. and Yang, G. (2019). Phosphorus sorption behavior on sediments in Sanggou Bay related with their compositions by sequential fractionation. *Ecotoxicol. Environ. Saf.*, 169, 144-149.

6. Hei, P., Zhang, Y., Shang, Y., Lei, X., Quan, J. and Zhang, M. (2017). An approach to minimizing the uncertainty caused by sediment washing pretreatment in phosphorus adsorption experiments. *Ecol. Eng*., 107, 244-251.

7. Huang, W., Lu, Y., Li, J.H., Zheng, Z., Zhang, J.B. and Jiang, X. (2015). Effect of ionic strength on phosphorus sorption in different sediments from a eutrophic plateau lake. *RSC Adv*., 5, 79607-79615.

8. Huang, S., Huang, H. and Zhu, H. (2016). Effects of the addition of iron and aluminum salt on phosphorus adsorption in wetland sediment. *Environ. Sci. Pollut. Res.*, 23, 10022-10027.

9. Li, M., Whelan, M.J., Wang, G.Q. and White, S.M. (2013). Phosphorus sorption and buffering mechanisms in suspended sediments from the Yangtze estuary and Hangzhou bay, China. *Biogeosci.*, 10, 3341-3348.

10. Meng, J., Yao, Q. and Zhigang, Y. (2014). Particulate phosphorus speciation and phosphate adsorption characteristics associated with sediment grain size. *Ecol. Eng.*, 70, 140-145.

11. Bai, J., Ye, X., Jia, J., Zhang, G., Zhao, Q., Cui, B. and Liu, X. (2017). Phosphorus sorption-desorption and effects of temperature, pH and salinity on phosphorus sorption in marsh soils from coastal wetlands with different flooding conditions. *Chemosphere*, 188, 677-688.

12. Kwak, D-K., Jeon, Y-T. and Hur, Y. D. (2018). Fractionation and release characteristics of Sediment in the Saemangeum Reservoir for seasonal change. *Inter. J. Sediment Res.*, 33(3), 250-261.

13. Mendes, L.R.D., Tonderski, K. and Kjaergaard, C. (2018). Phosphorus accumulation and stability in sediments of

surface-flow constructed wetlands. *Geoderma*, 331, 109-120.

14. Xiao, Y., Xia, Y., Yuan, S-y. and Tang, H-w. (2017). Flow structure and phosphorus adsorption in bed sediment at a 90° channel confluence. *J. Hydrodyn. (Ser. B)*, 29 (5), 902-905.

15. Zhu, J., Li, M., and Whelan, M. (2018). Phosphorus activators contribute to legacy phosphorus availability in agricultural soils: A review. *Sci. Tot. Environ.*, 612, 522-537.

16. Han, C., Wang, Z., Yang, W., Wu, Q., Yang, H. and Xue, X. (2016). Effects of pH on phosphorus removal capacities of basic oxygen furnace slag. *Ecol. Eng.*, 89, 1-6.

17. Li, Z.R., Sheng, Y.Q., Yang, J. and Burton, E.D. (2016). Phosphorus release from coastal sediments: impacts of the oxidation-reduction potential and sulfide. *Mar. Pollut. Bull.*, 113, 176-181.

18. Yao M.K., Brou, Y.S., Trokourey, A. and Soro, M.B (2017). Metal Pollution and Ecological Risk Assessment in Sediment of Artificial Estuary: Case of Vridi Channel, Côte d'Ivoire. *J. Appl. Sci. Environ. Manage.*, 21 (4), 785-792.

19. Yao, M.K. and Trokourey, A. (2018). Fractionation distribution and ecological risk assessment of some trace metals in artificial estuary: Vridi channel (Côte d'Ivoire). *Adv. Nat. Appl. Sci.*, 12(6), 1-6.

20. Yao, M.K. and Trokourey, A. (2018). Influence de l'hydroclimat sur la dynamique saisonnière de certains éléments traces métalliques dans un estuaire marin : Cas d'étude. *J. Soc. Ouest-Afr. Chim.*, 045, 31-41.

21. N'Da, S., Yao, M.K. and Trokourey, A. (2018). Seasonal dynamics of phosphorus fractions in artificial marine estuary: Vridi channel (Côte d'Ivoire). *Inter. J. Adv. Biol. Res.*,8 (4), 458-469.

22. Affian Koudio (2003). Approche environnementale d'un écosystème lagunaire microtidal (la lagune Ebrié en Côte d'Ivoire), par des études géochimiques et hydrologiques, bathymétriques et hydrologiques : contribution du S.I.G. et de la télédétection. Thèse de doctorat d'état, Université de Cocody, Abidjan, Côte d'Ivoire, pp. 1- 225.

23. Gnagne, Y.A., Yapo, B.O., Meité, L., Kouamé, V.K., Gadji, A.A., Mambo, V. and Houenou, P. (2015). Caractérisation physico-chimique et bactériologique des eaux usées brutes du réseau d'égout de la ville d'Abidjan. *Int. J. Biol. Chem. Sci.*, 9(2), 1082-1093.

24. AFNOR X 31-100 standard (1992). Qualité des sols-échantillonnage, méthode de prélèvement d'échantillons de sols. Boutique AFNOR Edition Décembre 1992, France.

25. AFNOR NF EN ISO 16720 standard (2007). Qualité du sol-prétraitement des échantillons par lyophilisation pour analyse subséquente. Mai 2007, France.

26. Murphy, J. and Riley, J.P. (1962). Amodified single solution method for determination of phosphate in natural waters. *Anal. Chim. Acta* , 27, 31-36.

27. AFNOR NF T90-023 standard (1982). Essai des eaux, dosage des orthophosphates, des polyphosphates et du phosphore total. Recueil de Normes Françaises, Qualité de l'eau, environnement 1994, pp. 356-366. ISBN: 212-17-9011 X

28. Dubus Igor (1997). Étude au laboratoire de la rétention du phosphore dans les sols ferralitiques allitiques de l'île de Maré. Convention Sciences de la Vie-Agropédologie (N°40), ORSTOM editions, île de loyauté, Maré, Nouvelle Calédonie, pp. 1-43. Identifiant IRD: fdi 010011063.

29. Lagergren, S. (1898). About the Theory of So-Called Adsorption of Soluble Substances. *Kungliga Svenska Vetenskapsakademiens Handlingar*, 24,1-39.

30. Blanchard, G., Maunaye, M. and Martin, G. (1984). Removal of heavy metals from waters by means of natural zeolites. *Water Res*., 18, 1501-1507.

31. Díaz-Blancas, V., Ocampo-Pérez, R., Leyva-Ramos, R., Alonso-Dávila, P.A. and Moral-Rodríguez, A.I. (2018). 3D modeling of the overall adsorption rate of metronidazole on granular activated carbon at low and high concentrations in aqueous solution. *Chem. Eng. J.*, 349, 82-91.

32. Wu, T., Wang, Z., Tong, Y., Wang, Y. and Loon, L.R.V. (2018). Investigation of Re (VII) diffusion in bentonite by through-diffusion and modeling techniques. *Appl. Clay Sci.*, 166, 223-229.

33. Weber, W.J. and Morris, J.C. (1963). Kinetics of adsorption on carbon from solution. *J. Sanit. Eng. Div. Am. Soc. Civ. Eng*., 89, 31-60.

34. Giles, C.H., MacEwan, T.H., Nakhwa, S.N. and Smith, D. (1986). Studies in adsorption, 1986 (Part XI). A system of classification of solution adsorption isotherms, and its use in diagnosis of adsorption mechanisms and in measurements of specific surface areas of solids. *J. Chem. Soc.*, 10, 3973-3993.

35. Brunauer Stephen (1943). The adsorption of gases and vapors. Volume I, Physical. Adsorption, Oxford University press, United States, pp. 1-511. https://doi.org/10.1021/ed021p52.1- ASIN: B005KDFW5K

36. Langmuir, I. (1938). The adsorption of gases on plane surfaces of glass, mica and platinum. *J. Am. Chem. Soc*., 40(9), 1361-1403.

37. Hall, K.R., Eagleton, L.C., Acrivos, A. and Vermeulen, T. (1966). Pore and soliddiffusion kinetics in fixed-bed adsorption under constant-pattern conditions. *Ind. Eng. Chem. Fund.*, 5, 212–223.

38. Freundlich, H. (1906). On adsorption in solution. *Z. Physik. Chem*., 57, 385-471.

39. Coulibaly, S. L. (2014). Abattement des phosphates des eaux usées par adsorption sur des géomatériaux constitués de Latérite, grès et schistes ardoisiers. (Doctoral dissertation, Université de Lorraine). pp.1-213

40. Chmielewska, E., Hodossyova, R. and Bujdos, M. (2013). Kinetic and thermodynamic studies for phosphate removal using natural adsorption Materials. *Pol J. Environ Stud.*, 22(5), 1307–1316.

41. Hou, Q., Meng, P., Pei, H., Hu, W. and Chen, Y. (2018). Phosphorus adsorption characteristics of alum sludge: Adsorption capacity and the forms of phosphorus retained in alum sludge. *Mat. Lett.*, 229, 31-35.

42. Fang, H., Cui, Z., He, G., Huang, L. and Chen, M. (2017). Phosphorus adsorption onto clay minerals and iron oxide with consideration of heterogeneous particle morphology. *Sci. Tot. Environ.*, 605–606, 357-367.

43. Lin, L., Li, Z., Song, X., Jiao, Y. and Zhou, C. (2018). Preparation of chitosan/lanthanum hydroxide composite aerogel beads for higher phosphorus adsorption. *Mat. Lett.*, 218, 201-204.

44. Chaussidon, J. (1958). sur la notion de double couche diffuse. *Bull. Groupe fr. Argiles*, 10(5), 27-30.

45. Liu, M., Hou, L., Xu, S., Ou, D., Yang, Y., Zhang, B. and Liu, Q. (2002). Adsorption of phosphate on tidal flat surface sediments from the Yangtze Estuary. *Environ. Geol.*, 42 (6), 657-665.

46. Djelloul Claude (2014). Expérimentation, modélisation et optimisation des effluents textiles. Thèse de Doctorat. Université de Mohamed Khider de Biskra, République d'Algérie, pp. 1-116.

47. Karaca, S., Gürses, A., Ejder, M. and Açikyildiz, M. (2004). Kinetic modeling of liquid-phase adsorption of phosphate on dolomite. *J. colloid. interface Sci.*, 277(2), 257-263.

48. Masmoudi, T., Guergazi, S. and Achour, S. (2018). Élimination du mercure par le charbon actif. *Larhyss J.*, 34, 21-38.

49. Ouakouak, A.K. and Youcef, L. (2016). Adsorption des ions Cu2+ sur un charbon actif en poudre et une bentonite sodique. *Larhyss J.*, 27, 39-61.

50. Barrow N.J. (1990). Relating chemical processes to management systems. Proceedings of Phosphorus requirements for sustainable agriculture in Asia and Oceania, Manilla, Philippines. 6th-10th March. Pp. 199-209.

51. Rahman, M., Adil, M., Yusof A. M., Kamaruzzaman, Y.B. and Ansary, R.H. (2014). Removal of Heavy Metal Ions with Acid Activated Carbons Derived from Oil Palm and Coconut Shells. *Mat.*, 7, 3634-3650.

52. Jiang, M., Jin, X., Lu, X. and Chen, Z. (2010). Adsorption of Pb (II), Cd (II), Ni (II) and Cu(II) onto natural kaolinite clay. *Desalination*, 252(1-3), 33–39.